THE STRATIGRAPHY OF MERCURY'S CRUST AS EXPOSED BY IMPACT CRATERS: A GLOBAL CLASSIFICATION. J. M. Leeburn[1,2], B. W. Denevi[2], C. M. Ernst[2], and R. L. Klima[2], [1]Department of Geology and Environmental Science, Wheaton College, Wheaton, IL 60187, USA (Jeffrey.Leeburn@my.wheaton.edu), [2]Johns Hopkins University Applied Physics Laboratory, Laurel, MD 20723, USA.

Introduction: Understanding the origin and evolution of Mercury's crust was a key goal of the MESSENGER mission. Prior to MESSENGER's exploration of Mercury, a leading hypothesis for the formation of the planet's crust was through crystal–liquid fractionation of a magma ocean, leading to a plagioclase flotation crust analogous to that of the Moon [e.g., 1–3]. However, reflectance observations [4,5] and elemental abundance data [6,7] make it clear that Mercury's crust is very different from the Moon's, and interpretations based on the planet's geomorphology and crater size–frequency distributions imply widespread resurfacing occurred, likely through a combination of volcanism and impact cratering [e.g., 8–14]. This geologic activity complicates an examination of Mercury's early crust.

Here we investigate Mercury's stratigraphy as exposed by impact craters >20 km in diameter in order to evaluate the mode(s) of formation of a key crustal unit, the low-reflectance material (LRM) [15–17]. LRM has been documented to be mainly exposed from depth, and proposed to be at the bottom of the stratigraphic column, either as a component of the lower crust or upper mantle [e.g., 18,19]. The reflectance of LRM is up to ~30% below the global mean, and it has a shallower (bluer) spectral slope, with a broad absorption-band-like feature at ~600 nm [16,17]. These properties together with thermal neutron measurements have led to the interpretation that LRM is rich in graphite (up to 5 wt.%) [16,20]. Geochemical modeling has also shown that graphite is the only mineral that would have been buoyant in a magma ocean, suggesting it may have been a component in the earliest-forming crust [21]. We explore whether the global occurrences and regional variations of LRM are consistent with this scenario, and investigate the role of early volcanism in the formation of Mercury's crust.

Methodology: We examined the spectral properties of craters >20 km in diameter using the crater catalog of Fassett et al. [11], and the degradation states assigned to these craters by Kinczyk et al. [22]. Working from least to most degraded, we inspected each crater's ejecta deposit and central structure (typically a central peak) to determine whether LRM was present or absent. This assessment was made using an enhanced color product created from a principal components (PC) analysis of the global eight-color mosaic from the Mercury Dual Imaging System (MDIS) wide-angle camera (WAC), where the second and first PC are displayed in red and green, respectively, and a ratio of images acquired at 430 nm and 1000 nm is displayed in blue (Fig. 1). Higher-resolution regional color products were also used, where available. The depth of origin of spectrally distinct material was estimated by calculating the maximum depth of excavation for ejecta and the minimum depth of origin (equal to the maximum depth of impact melting) for central peaks [18,19].

Results: It was possible to definitively assess the presence or absence of LRM for 1,019 of the 7,450 craters >20 km in the global catalog. The majority of those craters for which no determination was possible were highly degraded with no distinct ejecta deposit, and subdued or absent central structures; a minority were excluded due to poor color data quality such as near the poles where incidence angles were high.

From this dataset, the global median depth of origin for LRM is 4.3 km, compared to 3.1 km for craters with no LRM (Fig. 2A). A histogram of the depths of occurrence for LRM suggests we are observing the mode, whereas for non-LRM, each bin increases toward the minimum values we observe (Fig. 2A), indicating the median value for non-LRM is likely an overestimate due to the cutoff diameter of 20 km used in our study. We examined regional subsets of the global catalog, including smooth plains such as the well studied Caloris Planitia (Fig. 2B) [19]. While smooth plains often have a relatively small number of

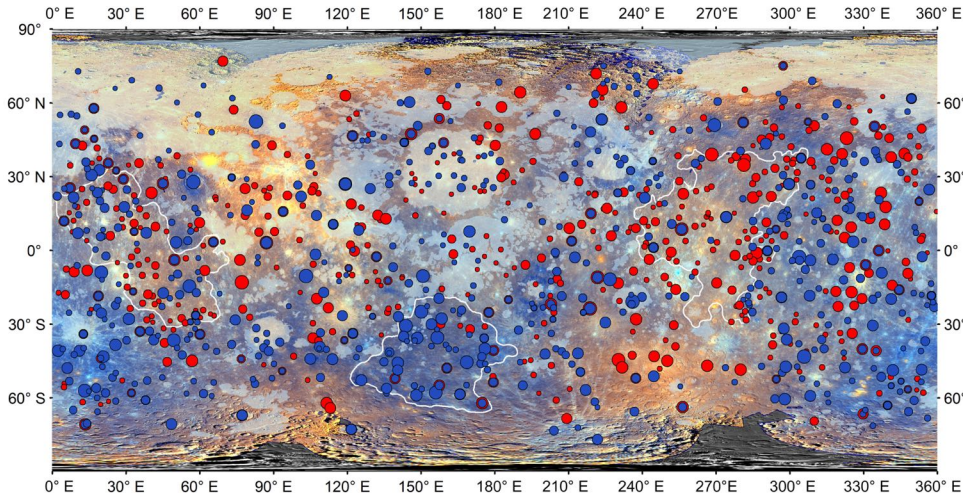

Figure 1. Global catalog of craters >20 km in diameter that expose LRM (blue symbols) and those that do not (red). The symbol size is shown proportional to the material's depth of origin and ranges from 1.4 km to 35 km (materials originating from depths >35 km excluded). Two intercrater plains regions (30° E, 270° E) and an area with a high concentration of LRM (160° E) are outlined in white [23,24], smooth plains (transparent white) are shown over an MDIS WAC enhanced color mosaic (see text for desciption).

craters >20 km in diameter, their histogram typically resembles that of the global population, with median LRM depths of origin ~3-4 km, and shallower depths where LRM is absent.

Three additional regions were examined: two areas of intercrater plains, and a region south of Caloris that has the highest density of craters >65 km in diameter, and a high concentration of LRM [23,24]. The first area of intercrater plains (30° E, Fig. 1) has been proposed to be a region where intercrater plains of volcanic origin largely bury two impact basins [23,24]. The histogram of depths of origin in this region (Fig. 2C) resembles both the global population and smooth plains such as within the Caloris basin. The second region of intercrater plains (270° E, Fig. 1) is distinct from all areas examined in terms of both the dearth of craters that expose LRM, and the larger median depth of origin for LRM (5.7 km) (Fig. 2D). Finally, the LRM-rich region previously identified [23,24] includes a higher density of craters that expose LRM across all diameters, and has few craters that do not expose LRM (Fig. 2E). Craters that do not expose LRM appear to have formed within small patches of smooth plains within this region.

Discussion: Interpretations of this dataset are complicated by the fact that large craters that excavate to great depths are relatively rare, and our sample is thus strongly biased toward those that sample only the upper few km. However, global and regional trends reveal that the distribution of LRM is widespread but heterogenous (Fig. 1), and occurs at greater median depths than craters that lack LRM (Fig. 2). Craters that do not expose LRM indicate there are regions of the crust that lack LRM even at relatively large depths, up to a maximum of 23 km. The depths of origin materials within many regions of smooth (e.g., Fig. 2B) and intercrater (Fig. 2C) plains are similar, suggesting they are stratigraphically similar and, consistent with other geologic evidence [e.g., 8,9,14,24], share a common volcanic origin.

Differences from the global trend may also be informative. The intercrater plains region near 270° E stands out for its lack of LRM (Fig. 2D); this area also largely corresponds to a region of high Mg [25]. This may be an area where LRM does not generally occur at depth, or LRM resides only at greater than average depths; its distinct stratigraphy and composition point to a unique regional geolgoic history. Our results for the LRM-rich region south of Caloris (Fig. 2E) are consistent with past work suggesting this region experienced little volcanic resurfacing, and remnants of the early crust may be exposed [23,24].

The global picture provided by this dataset is consistent with an early low-reflectance crust, such as would have formed from the flotation of graphite in a magma ocean [21]. However, relatively low concentrations of graphite, even in LRM [16,20], the heterogeneous distribution of LRM observed here, and the largely overlapping depths of origin of LRM and material of higher reflectance are consistent with disruption, mixing, and burial by volcanism and impact events.

References: [1] Adams J.B. and McCord T.B. (1977) *Bull. Am. Astron. Soc.*, *9*, 457. [2] Blewett D.T. et al. (1997) *Icarus*, *129*, 217–231. [3] Blewett D.T. et al. (2007) *JGR*, *112*, 10.1029/2006JE002713. [4] Denevi B.W. and Robinson M.S. (2008) *Icarus*, *197*, 239–246. [5] Braden S.E. and Robinson M.S. (2013) *JGR:Planets*, *118*, 1903–1914. [6] Nittler L.R. et al. (2011) *Science*, *333*, 1847–1850. [7] Weider S.Z. et al. (2012) *JGR*, *117*, 10.1029/2012JE004153. [8] Strom R.G. (1977) *Phys. Earth Planet. Int.*, *15*, 156–172. [9] Denevi B.W. et al. (2009) *Science*, *324*, 613–618. [10] Denevi B.W. et al. (2013) *JGR: Planets*, *118*, 891–907. [11] Fassett C.I. et al. (2011) *GRL*, *38*, 10.1029/2011GL047294. [12] Strom R.G. et al. (2011) *PSS*, *59*, 1960–1967. [13] Marchi S. et al. (2013) *Nature*, *499*, 59–61. [14] Whitten J.L. et al. (2014) *Icarus*, *241*, 97–113. [15] Robinson M.S. et al. (2008) *Science*, *321*, 66–69. [16] Murchie S.L. et al. (2015) *Icarus*, *254*, 287–305. [17] Klima R.L. et al. (2016) *LPSC 47*, Abs. 1195. [18] Ernst C.M. et al. (2010) *Icarus*, *209*, 210–223. [19] Ernst C.M. et al. (2015) *Icarus*, *250*, 413–429. [20] Peplowski P.N. et al. (2016) *Nature Geoscience*, 9, 273–276. [21] Vander Kaaden K.E. and McCubbin F.M. (2015) *JGR: Planets*, *120*, 195–209. [22] Kinczyk M.J. et al. (2016) *LPSC 47*, Abs. 1573. [23] Denevi B.W. et al. (2016) *LPSC 47*, Abs. 1624. [24] Denevi B.W. et al. (2017) Solomon S.C., Nittler L.R., Anderson B.J., editors, in *Mercury: The view after MESSENGER* (Cambridge, UK: Cambridge Univ. Press), in press. [25] Weider S.Z. et al. (2015) *Earth and Planetary Science Letters*, *416*, 109–120.

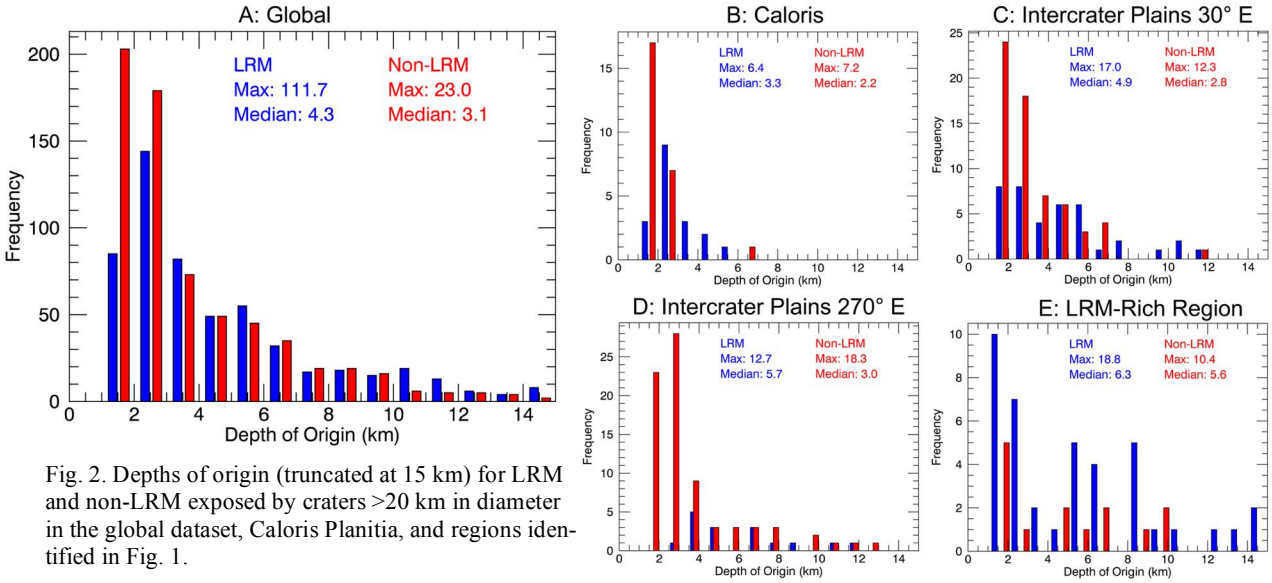

Fig. 2. Depths of origin (truncated at 15 km) for LRM and non-LRM exposed by craters >20 km in diameter in the global dataset, Caloris Planitia, and regions identified in Fig. 1.